Quantum three-coloring dimer model and the disruptive effect of quantum glassiness on its line of critical points

Claudio Castelnovo,[1] Claudio Chamon,[1] Christopher Mudry,[2] and Pierre Pujol[3]
[1]*Physics Department, Boston University, Boston, Massachusetts 02215, USA*
[2]*Paul Scherrer Institut, CH-5232 Villigen PSI, Switzerland*
[3]*Laboratoire de Physique, Groupe de Physique, Théorique de l'École Normale Supérieure, Lyon, France*
(Received 3 March 2005; revised manuscript received 2 June 2005; published 2 September 2005)

We construct a quantum extension of the (classical) three-coloring model introduced by Baxter [J. Math. Phys. **11**, 784 (1970)] for which the ground state can be computed exactly along a continuous line of Rokhsar-Kivelson solvable points. The quantum model, which admits a local spin representation, displays at least three different phases; an antiferromagnetic phase, a line of quantum critical points, and a ferromagnetic phase. We argue that, in the ferromagnetic phase, the system cannot reach dynamically the quantum ground state when coupled to a bath through local interactions, and thus lingers in a state of quantum glassiness.

DOI: 10.1103/PhysRevB.72.104405 PACS number(s): 75.10.Jm, 05.30.−d, 05.70.Jk, 64.70.Pf

I. INTRODUCTION

It has long been known that strongly correlated electronic systems at zero temperature can be parametrically close to fixed points with macroscopically degenerate ground state manifolds. This is so for a two-dimensional degenerate electron gas in the quantum Hall regime for which the largest energy scales are the cyclotron and Zeeman splittings, and for Mott insulators when the Coulomb energy in the form of an on-site repulsive Hubbard U dominates all other energy scales.[1,2] Similarly, the zero temperature phase diagram of a class of quantum dimer models and geometrically frustrated quantum systems are known to be influenced by fixed points with massively degenerate ground state manifolds.[3] Whereas most of the efforts have been directed toward exploring the nature of the collective excitations present in the different phases and at their boundaries, relatively little attention has been paid to nonequilibrium phenomena induced by the coupling to a bath. The goal of this paper is to illustrate how quantum glassiness can emerge in a two-dimensional homogeneous quantum system *whose local degrees of freedom are subjected to a strong constraint*, when the system is coupled to a bath. In the process, we also show how to obtain a whole line of solvable Rokhsar-Kivelson (RK) points in a hard-constrained quantum system.

More specifically, we are going to construct a quantum version of the (classical) three-coloring model introduced by Baxter in Ref. 4 which we shall call the quantum three-coloring dimer model. We find that: (i) For any value of a dimensionless coupling βJ the ground state follows from taking a superposition of states in a preferred basis of the Hilbert space. The dependence on βJ of the normalization of the ground state defines the partition function of a generalization of the classical three-coloring model at the reduced inverse temperature βJ.[5–7] (ii) The excitation spectrum above the ground state is identical to the spectrum of relaxation times of a classical rate equation that depends on a dimensionless parameter α in addition to βJ. (iii) The ground state expectation value of any two local operators at unequal points in space and imaginary time can be interpreted as the classical correlation function of the classical three-coloring model endowed with dynamical rules, provided both operators are diagonal in the preferred basis. This interplay between a quantum model and a classical stochastic model generalizes a similar connection established by Henley for the square lattice quantum dimer model.[8] (iv) The quantum three-coloring dimer model is *local* in that it can be interpreted as a Hamiltonian for quantum spins whose interactions have a *finite* range as long as the parameter α remains nonnegative. In the spin representation, the zero-temperature phase diagram has at least three phases, an antiferromagnetic (AF) phase when $-\beta J \gg 1$, a line of quantum critical points in the neighborhood of infinite temperature and a ferromagnetic (F) phase when $\beta J \gg 1$. (v) We argue that, in the F phase, the relaxation time needed for a generic initial state to decay to the ground state through a *local* coupling to a bath diverges exponentially with the system size, a property that signals quantum glassiness.[9]

II. DEFINITION OF THE QUANTUM THREE-COLORING MODEL

The classical three-coloring model is a model of dimers laid down on the bonds of a lattice with coordination number 3. More precisely, the dimers come in three kinds (or colors), A, B, and C and occupy the bonds $\langle ij \rangle$ between nearest-neighboring sites i and j of the honeycomb lattice according to two rules: (1) all bonds are occupied (close-packed constraint); and (2) all three dimers meeting at a site (vertex) are different (three-coloring constraint). The classical phase space is thus the set $\mathcal{S}$ of all configurations $\mathcal{C}$ obtained by coloring the bonds of the honeycomb lattice in any of the three colors A, B, C with the condition that three bonds meeting at a site have different colors. Two possible configurations $\mathcal{C}_{AF}$ and $\mathcal{C}_{F}$ are depicted in Fig. 1.

To any configuration $\mathcal{C} \in \mathcal{S}$ there corresponds a unique configuration $\{\sigma_i\}$ of Ising degrees of freedom $\sigma_i = \pm$, defined on the sites i of the honeycomb lattice, whereby $\sigma_i = +(-)$ if the three dimers meeting at i can be obtained from ABC

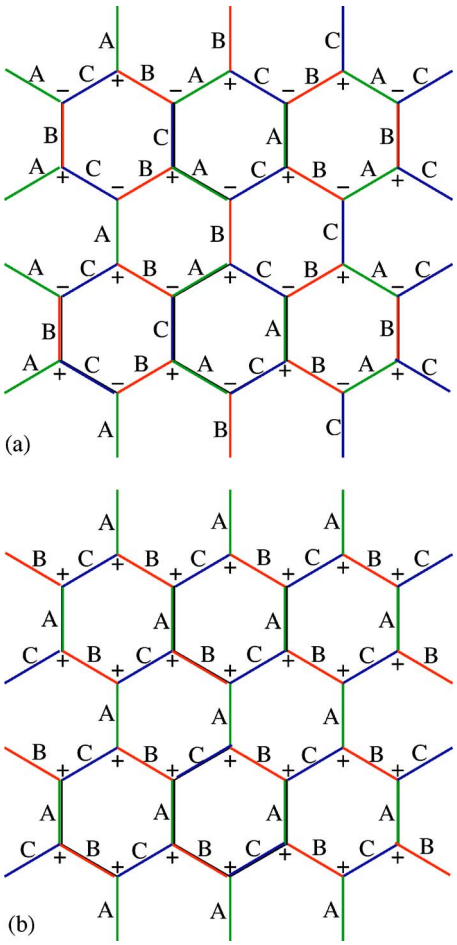

FIG. 1. (Color online) Two configurations, $\mathcal{C}_{AF}$ in panel (a) and $\mathcal{C}_F$ in panel (b), from the three-coloring model.

through an even (odd) permutation when moving clockwise around i. The configuration $\mathcal{C}_{AF}$ ($\mathcal{C}_F$) in Fig. 1 thus corresponds to an AF (F) configuration of the Ising spins. Evidently, any global even permutation of the colors ABC leaves the Ising configuration unchanged. Hence there is a three-to-one relation between $\mathcal{S}$ and the set of all Ising spin configurations on the honeycomb lattice such that the magnetization along the perimeter of any elementary hexagon is either 0 as in Fig. 1(a) or ±6 as in Fig. 1(b).[10]

Another useful characterization of a configuration $\mathcal{C} \in \mathcal{S}$ is in terms of *two-color paths*, each of which is defined by drawing a line along all bonds colored in any given two (say B or C) of the three colors that initiate from a site (the seed) and by specifying the color pattern (say $BCBC\ldots$ or $CBCB\ldots$) along the line. Upon imposing periodic boundary conditions one can interpret a configuration $\mathcal{C} \in \mathcal{S}$ as a set of two-color closed paths (where the same two colors have been chosen for all the paths in the lattice) that are nonintersecting and close-packed. We will refer to such objects making up a configuration $\mathcal{C} \in \mathcal{S}$ as *loops*. For example, configuration $\mathcal{C}_{AF}$ ($\mathcal{C}_F$) in Fig. 1 can be viewed as being made solely of loops of maximal (minimal) nonnegative curvature.

We will denote by ℓ a *decorated loop*, i.e., an object made of all $2L_\ell$ independent colored bonds emanating from the L_ℓ sites through which a loop passes, and by the set of its colored dangling bonds, as defined hereafter (see also Fig. 2). For any ℓ, the L_ℓ bonds that alternate between the colors B and C, say, form the backbone of ℓ, while the remaining L_ℓ bonds of color A that stick out of the backbone connect the loop to its dangling bonds, i.e., the two bonds that depart from the free end of each A colored bond. The definition of a decorated loop therefore encodes the information about the colors of all the dangling bonds of the loop. The reasons for such a choice will become evident as we proceed with the formulation of our quantum model [see Eq. (1f) and thereafter]. The set of all possible decorated loops is $\mathcal{L}$. Configuration $\mathcal{C}_{AF}$ in Fig. 1 is made exclusively of objects ℓ with six connecting bonds (i.e., the bonds joining the loop backbone to the dangling bonds) of color A, B, and C, respectively. Configuration $\mathcal{C}_F$ in Fig. 1 is made exclusively of objects ℓ with L connecting bonds of color A, B, and C, respectively, where L is the linear size of the system.

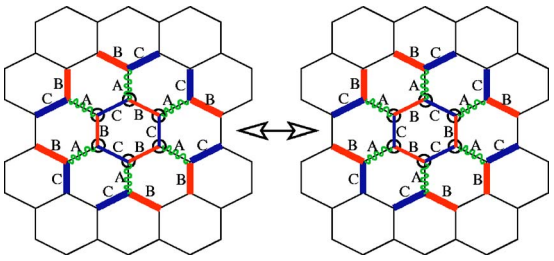

FIG. 2. (Color online) Two examples of decorated loops of the types $BCBC\ldots$ and $CBCB\ldots$ in the three-coloring model are shown. They are related by the color-swap defined in the text. Notice the information encoded in both loops, (1) the backbone structure (circled lattice sites) that is specified by all the sites visited by the sequence of bonds of color B or C emanating from a seed, (2) the two-color pattern ($BCBC\ldots$ and $CBCB\ldots$) along each loop, and (3) the colors and locations of all the dangling bonds (thick lines). The connecting bonds that link the backbone of a decorated loop to its dangling bonds are represented by wavy lines for clarity.

By specifying the colors and the locations of both the connecting and the dangling bonds, one identifies two decorated loops ℓ and $\bar{\ell}$ related by the *color-swap* operation $B \leftrightarrow C$ along the L_ℓ bonds making up the loop backbone. This color swap relating two *different* configurations $\mathcal{C}$ and $\bar{\mathcal{C}}$ in $\mathcal{S}$ is illustrated in Fig. 2. Given a decorated loop ℓ and a configuration $\mathcal{C}$, it is always possible to decide if ℓ belongs to $\mathcal{C}$, i.e., either $\ell \in \mathcal{C}$ or $\ell \notin \mathcal{C}$. By construction: (1) If $\ell \in \mathcal{C}$ then $\bar{\ell} \notin \mathcal{C}$. (2) If $\ell \in \mathcal{C}$ then there exists a unique configuration $\bar{\mathcal{C}}$ (to which $\bar{\ell}$ belongs) obtained by the color swap operation along the backbone of ℓ in $\mathcal{C}$.

To define the quantum three-coloring dimer model we need a Hilbert space and a Hamiltonian. The Hilbert space is the span of all orthonormal states $|\mathcal{C}\rangle$ labeled by the classical configurations $\mathcal{C} \in \mathcal{S}$. The Hamiltonian, which we show below to be of the RK type, takes the form

$$\hat{H}_{RK} := \sum_{\ell \in \mathcal{L}} w_\ell \hat{Q}_\ell, \tag{1a}$$

$$\hat{Q}_\ell := \hat{V}_\ell - \hat{T}_{\ell,\bar{\ell}}, \tag{1b}$$

where the potential and kinetic energy operators are

$$\hat{V}_\ell := e^{-\beta J \varepsilon_\ell/2} \hat{P}_\ell \equiv e^{-\beta J \varepsilon_\ell/2} \sum_{\mathcal{C} \in \mathcal{S}} c_\ell |\mathcal{C}\rangle\langle\mathcal{C}|, \tag{1c}$$

$$\hat{T}_{\ell,\bar{\ell}} := \sum_{\mathcal{C} \in \mathcal{S}} c_\ell |\bar{\mathcal{C}}\rangle\langle\mathcal{C}|, \tag{1d}$$

respectively. The dimensionless coupling βJ is real valued and $c_\ell = 1$ if $\ell \in \mathcal{C}$, while it vanishes otherwise. The dimensionless energy

$$E_\mathcal{C} := -\sum_{\langle ij \rangle} \sigma_i \sigma_j \tag{1e}$$

is the classical energy of the Ising spin configuration $\{\sigma_i\}$ associated to $\mathcal{C}$ in units of $|J|$. Finally, the dimensionless energy

$$\varepsilon_\ell = E_{\bar{\mathcal{C}}} - E_\mathcal{C} \tag{1f}$$

is uniquely defined for any $\mathcal{C} \in \mathcal{S}$ that contains ℓ. Notice that the definition of a decorated loop was precisely chosen so that the energy difference $E_{\bar{\mathcal{C}}} - E_\mathcal{C}$ depends only on the information contained in ℓ, and not on further details of $\mathcal{C}$ and $\bar{\mathcal{C}}$.

Whatever the choice made for the energy scales $\{w_\ell \geqslant 0\}$, the wave function

$$|\Psi_{RK}\rangle = \sum_{\mathcal{C} \in \mathcal{S}} \exp(-\beta J E_\mathcal{C}/2) |\mathcal{C}\rangle \tag{2a}$$

is the ground state of $\hat{H}_{RK}$, as follows from the facts that: (1) $\hat{Q}_\ell^2$ is proportional to $\hat{Q}_\ell$, and (2) $|\Psi_{RK}\rangle$ is annihilated by $\hat{Q}_\ell$ $(\forall \ell \in \mathcal{L})$. Remarkably, the normalization of $\langle\Psi_{RK}|\Psi_{RK}\rangle$ is nothing but the partition function

$$Z := \sum_{\mathcal{C} \in \mathcal{S}} e^{-\beta J E_\mathcal{C}} \tag{2b}$$

of the generalized three-coloring model (see Refs. 5–7) with the configuration energy (1e), i.e., up to a multiplicative factor of 3, it is the partition function of the nearest-neighbor Ising model on the honeycomb lattice with the *local constraint* that the magnetization on any elementary hexagon is 0 or ± 6.[10] The zero-temperature phase diagram of the quantum three-coloring model along the axis $\beta J \in \mathbb{R}$ *contains* the phase diagram of the generalized classical three-coloring model along the reduced temperature axis $\beta J \in \mathbb{R}$.

III. PHASE DIAGRAM OF THE CLASSICAL THREE-COLORING MODEL

The partition function (2b) was evaluated by Baxter at infinite temperature.[4] Through a height representation of the three-coloring model, it was shown in Ref. 11 that at infinite temperature the probability that two points of the honeycomb lattice separated by a distance r belong to the same loop decays with r algebraically and that this decay is captured by the $SU(3)_1$ Wess-Zumino-Witten (WZW) theory. The finite temperature phase diagram was studied numerically in Ref. 5 with a transfer matrix approach, in Ref. 6 with a cluster variational method (CVM), and in Ref. 7 using Monte Carlo simulations, the CVM, as well as perturbative renormalization-group (RG) techniques for infinitesimal values of the coupling βJ. The classical configuration that minimizes the energy $E_\mathcal{C}$ is the antiferromagnatic $\mathcal{C}_{AF}$ when $J < 0$ and the ferromagnetic $\mathcal{C}_F$ when $J > 0$ (see Fig. 1). Thermal fluctuations are expected to destroy both long-range ordered phases for a sufficiently large temperature. In view of the *local constraint* of the three-coloring model, the transition may be different in nature from the one of the unconstrained model. Numerical simulations are consistent with the termination of the F phase in a first order phase transition at the reduced temperature $(\beta J)_F$.[7] On the other hand, the $SU(3)_1$ WZW critical point at infinite temperature seems to be the end point of a line of critical points when $0 < \beta J \leqslant (\beta J)_{\rm cr}$. Whether $(\beta J)_{\rm cr} = (\beta J)_F$ or there exists intermediary phases[12,13] in the range $(\beta J)_{\rm cr} < \beta J < (\beta J)_F$ is not known at present. The phase diagram is not symmetric under $J \to -J$ as the *local constraint* favors the AF over the F state from an entropic point of view. The CVM predicts a critical end point $(\beta J)_{AF} < 0$ to the AF phase followed by a paramagnetic phase, possibly of the short-range resonating-valence-bond (RVB) type, that terminates in the critical point at infinite temperature. The conjectured phase diagram of the partition function (2b) is sketched in Fig. 3.

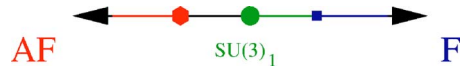

FIG. 3. (Color online) Conjectured phase diagram of the classical partition function (2b) along the reduced temperature axis βJ. The right end point of the AF phase is a hexagon. The left and right end points of the critical phase are a circle and a square, respectively. The circle corresponds to $\beta J = 0$ and realizes the $SU(3)_1$ WZW critical theory.

IV. EXCITATION SPECTRUM, LOCALITY, AND EMERGING TOPOLOGICAL QUANTUM NUMBERS

Although the ground state of $\hat{H}_{RK}$ does not depend on the choice of the couplings w_ℓ, the excitation spectrum does. We are now going to show that there exists a one-to-one correspondence between the excitation energies of $\hat{H}_{RK}$ and the relaxation modes of the three-coloring model endowed with the dynamics borrowed from a uniquely defined transition matrix $(W_{\mathcal{C}\mathcal{C}'})$. We begin by defining the matrix elements

$$W_{\mathcal{C}\mathcal{C}'} := -e^{-\beta J (E_\mathcal{C} - E_{\mathcal{C}'})/2} \langle \mathcal{C} | \hat{H}_{RK} | \mathcal{C}' \rangle. \tag{3a}$$

Although $(W_{\mathcal{C}\mathcal{C}'})$ is not symmetric in general, it shares the same set of eigenvalues as $\hat{H}_{RK}$. Furthermore it satisfies by construction the detailed balance condition

$$W_{\mathcal{C}\mathcal{C}'} e^{-\beta J E_{\mathcal{C}'}} = W_{\mathcal{C}'\mathcal{C}} e^{-\beta J E_\mathcal{C}} \tag{3b}$$

as well as the condition

$$0 = \sum_{\mathcal{C}' \in \mathcal{S}} W_{\mathcal{C}'\mathcal{C}}. \tag{3c}$$

Equation (3c) allows one to interpret the first order linear differential equation in imaginary time τ

$$\dot{p}_{\mathcal{C}}(\tau) = \sum_{\mathcal{C}' \in \mathcal{S}} W_{\mathcal{C}\mathcal{C}'} p_{\mathcal{C}'}(\tau) \tag{4}$$

as a master equation for the probabilities $\{p_{\mathcal{C}}(\tau)\}$ whose stationary solution is

$$p_{\mathcal{C}}^{(0)} = Z^{-1} \exp(-\beta J E_{\mathcal{C}}) \tag{5}$$

by Eq. (3b). Furthermore, the properly normalized ground state expectation value $\hat{G}_{\hat{B}\hat{A}}(\tau)$ of the product $\hat{B}(\tau) \times \hat{A}(0)$ at unequal imaginary times of any two operators $\hat{A}$ and $\hat{B}$ diagonal in the basis $|\mathcal{C}\rangle$ can be interpreted as a classical dynamical correlation function at unequal times:

$$\hat{G}_{\hat{B}\hat{A}}(\tau) = \sum_{\mathcal{C}'} \sum_{\mathcal{C}} B_{\mathcal{C}'} p_{\mathcal{C}'|\mathcal{C}}(\tau) A_{\mathcal{C}} p_{\mathcal{C}}^{(0)} \equiv G_{BA}(\tau). \tag{6}$$

The conditional probability $p_{\mathcal{C}'|\mathcal{C}}(\tau)$ is the solution to the master equation (4) with the initial condition $p_{\mathcal{C}'|\mathcal{C}}(\tau=0) = \delta_{\mathcal{C}'\mathcal{C}}$ while $B_{\mathcal{C}'}$ and $A_{\mathcal{C}}$ are the matrix elements of $\hat{B}$ and $\hat{A}$, respectively. Equation (6), relating classical stochastics of the three-coloring model to the quantum dynamics in imaginary time of the quantum three-coloring dimer model, is an example of a generic property of quantum dimer models at the so-called RK point as noted by Henley.[8]

We can now motivate our choice for the couplings w_ℓ,

$$w_\ell = w_0 f_\ell \exp[-\alpha(L_\ell - 6)]. \tag{7}$$

Here, the energy scale w_0 is of order 1. The number $0 < f_\ell \leqslant 1$ can always be chosen such that the classical stochastics in time encoded by Eq. (4) is the Glauber or Metropolis dynamics.[14] We do not believe this choice to be of consequence for spectral properties beyond the mean level spacing. The choice for the value of the dimensionless parameter α can affect spectral properties in a crucial way, however. Any $\alpha > 0$ implements (defines), in the thermodynamic limit, the condition of locality. A corollary to $\alpha > 0$ is the emergence of well-defined topological sectors in the thermodynamic limit.

The quantum three-coloring Hamiltonian (1) where the coupling constants w_ℓ are defined in Eq. (7) with $\alpha > 0$ is local in very much the same way as the effective quantum spin-1/2 model obtained from the expansion of the Hubbard model at half-filling, and in the limit of an on-site repulsion U much larger than the band width t. The potential energy (1c) associated with a decorated loop ℓ with perimeter L_ℓ generates 2, 3, …, L_ℓ-body Ising spin interactions for spins that can be as far as L_ℓ lattice spacings apart very much in the same way as ring exchange interactions along a closed path of length L_ℓ are induced to L_ℓ-th order in t/U for the Hubbard model at half-filling. In the case of both the quantum three-coloring and the effective Heisenberg model, these L_ℓ-body interactions are associated to characteristic energy scales that are exponentially suppressed with L_ℓ; namely, w_ℓ and $(t/U)^{L_\ell} \times t$, respectively. The same argument applies to the kinetic energy (1d). In fact, we shall show shortly that here the counterpart to the Hubbard model is the constrained transverse field Ising on the honeycomb lattice.

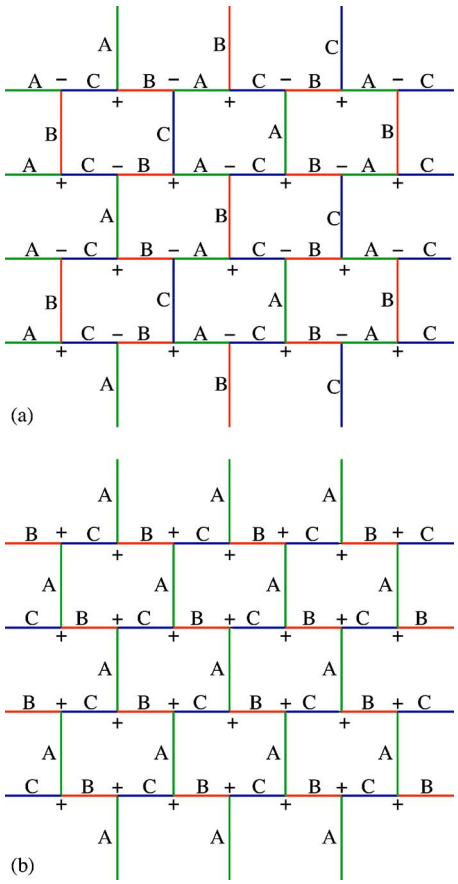

FIG. 4. (Color online) Two configurations $\mathcal{C}_{AF}$ in panel (a) and $\mathcal{C}_F$ in panel (b) in the brick wall representation. In panel (a) $N_A = N_B = N_C$. In panel (b) N_A is maximum with $N_B = N_C = 0$ for $\mathcal{C}_F$.

The concept of topological sectors is rooted in the following conservation laws characterizing any $\mathcal{C} \in \mathcal{S}$.[4] Choose the brick wall representation of the three-coloring model as depicted in Fig. 4. Draw a line between any two consecutive rows and count the number of intersections $N_{A,B,C}$ with vertical bonds of color A, B, and C, respectively. This triplet of numbers is independent of the choice of the two consecutive rows and characterizes globally each configuration $\mathcal{C} \in \mathcal{S}$. Furthermore, for any $\ell \in \mathcal{L}$ and for any $\mathcal{C} \in \mathcal{S}$ such that $\ell \in \mathcal{C}$, $N_{A,B,C} = \bar{N}_{A,B,C}$ whereby $N_{A,B,C}$ ($\bar{N}_{A,B,C}$) characterizes globally $\mathcal{C}$ ($\bar{\mathcal{C}}$), as long as ℓ is nonwinding. The numbers $N_{A,B,C}$ are elevated to the status of conserved quantum numbers under the quantum dynamics defined by $\hat{H}_{RK}$, provided $w_\ell = 0$ for all winding loops. In particular, these topological conservation laws emerge in the thermodynamic limit when $\alpha > 0$. It is possible that $0 \leqslant \beta J \leqslant (\beta J)_{\mathrm{cr}}$ realizes a line of quantum Lifshitz critical points when $\alpha > 0$,[15] with a dynamical exponent $z = 2$; this is in principle testable numerically.

V. QUANTUM THREE-COLORING MODEL AND THE CONSTRAINED QUANTUM ISING MODEL IN A TRANSVERSE FIELD

The RK three-coloring Hamiltonian (1a) is a special case of the Hamiltonian

$$\hat{H}_{3-c} := \sum_{\ell \in \mathcal{L}} w_\ell (v_\ell \hat{P}_\ell - t_\ell \hat{T}_{\ell,\bar{\ell}}), \tag{8}$$

where the dimensionless couplings v_ℓ and t_ℓ are real valued. The choice of the couplings $v_\ell = -\varepsilon_\ell J/(4w_\ell)$ and $t_\ell = 1$ implies that: (1) the matrix element

$$-(J/4)\sum_{\ell \in \mathcal{L}} \varepsilon_\ell \langle \mathcal{C}|\hat{P}_\ell|\mathcal{C}\rangle$$

is nothing but the classical Ising energy

$$-J\sum_{\langle ij\rangle} \sigma_i^z \sigma_j^z$$

of the nearest-neighbor Ising model on the honeycomb lattice subjected to the *local constraint on any elementary hexagon*[10]

$$\cos\left(2\pi \sum_{i \in \text{hex}} \sigma_i^z/3\right) = 1, \tag{9}$$

while (2) each term $w_\ell \hat{T}_{\ell,\bar{\ell}}$ is induced order by order in degenerate perturbation theory by the *small transverse field* $\Gamma\Sigma_i \sigma_i^x$. Here, it is the local constraint that is responsible for the macroscopic quasidegeneracy of the classical limit $\Gamma \to 0$ as opposed to the geometrical frustration in the Ising models treated in Ref. 16. This happens as long as the energy splitting of order J characteristic of the classical configurations that obey the three-coloring constraint is negligible compared to the very large characteristic energy U paid by any classical configuration that violates this constraint. The energy scale associated to the three-coloring constraint plays a role similar to that of a large Hubbard on-site repulsion for strongly correlated electrons or of the cyclotron energy in the regime of the fractional Hall effect. The constrained quantum Ising Hamiltonian in a small transverse field,

$$\hat{H}_{\text{Ising}} := \sum_{\ell \in \mathcal{L}} (-(J/4)\varepsilon_\ell \hat{P}_\ell - w_\ell \hat{T}_{\ell,\bar{\ell}}), \tag{10}$$

captures the $\mathbb{Z}_2$ quantum dynamics induced by time-reversal symmetry breaking in a triangular array of Josephson junctions when the superconducting order parameter breaks time-reversal invariance.[7,17] The quantum three-coloring Hamiltonians $\hat{H}_{3-c}$ and $\hat{H}_{RK}$ are also relatives to a model for quantum spin-1 degrees of freedom defined on the bonds of the honeycomb lattice introduced by Wen in Ref. 18.

We can now refine the notion of locality ($\alpha > 0$) of $\hat{H}_{RK}$. The quantum dynamics in real time of $\hat{H}_{RK}$ and of the constrained quantum Ising model $\hat{H}_{\text{Ising}}$ originate from the very same quantum tunneling processes between classical configurations. Their local nature is explicit in $\hat{H}_{\text{Ising}}$ and carries over to $\hat{H}_{RK}$.

VI. LOCAL COUPLING TO A THERMAL BATH, ARRESTED QUANTUM DYNAMICS, OR QUANTUM GLASSINESS

So far we have considered the quantum three-coloring model (8) or, equivalently, the constrained Ising model in a transverse field (10) in isolation. Energy is then a conserved quantum number and the real-time evolution of any state in the Hilbert space is a linear superposition of harmonics with frequencies $\omega_j = E_j/\hbar$ where the index j labels the exact eigenvalues of Hamiltonians (8) or (10).

In the spirit of Caldeira and Legget,[19] imagine coupling $\hat{H}_{\text{Ising}}$ ($\hat{H}_{RK}$) *very weakly* ($g_{i\lambda_i} \ll J, w_0$) to a bath of harmonic oscillators $\{a_{i,\lambda_i}^\dagger, a_{i,\lambda_i}\}$ through the *local* interactions[9]

$$\sum_{i\lambda_i} g_{i\lambda_i} \sigma_i^x (a_{i,\lambda_i} + \text{H.c}). \tag{11}$$

The effect of this phonon bath is to endow the energy eigenvalues of the strongly correlated system in isolation with finite lifetimes. These lifetimes can be calculated perturbatively. To put it differently, the presence of a phonon bath implies that we cannot consider a pure state, as was the case in deriving Eq. (6). The introduction of a density matrix is now required to study the thermodynamic behavior of $\hat{H}_{\text{Ising}}$ ($\hat{H}_{RK}$) and, in this sense, the evolution in real time of $\hat{H}_{\text{Ising}}$ ($\hat{H}_{RK}$) is better understood in terms of transition or relaxation rates between states of $\hat{H}_{\text{Ising}}$ ($\hat{H}_{RK}$) by absorption or emission of phonons. At zero temperature, any initial state of $\hat{H}_{\text{Ising}}$ ($\hat{H}_{RK}$) which is different from the ground state of $\hat{H}_{\text{Ising}}$ ($\hat{H}_{RK}$) can now decay to the ground state through spontaneous emission of phonons ($a_{i,\lambda_i}^\dagger$), i.e., by transferring energy to the thermal bath of harmonic oscillators. The goal of this section is to estimate the relaxation rate of an initial state of $\hat{H}_{\text{Ising}}$ ($\hat{H}_{RK}$) into the ground state of $\hat{H}_{\text{Ising}}$ ($\hat{H}_{RK}$) due to the coupling to the bath. It should be emphasized that these relaxation rates are completely unrelated to the imaginary-time dynamics of $\hat{H}_{RK}$ encoded by Eq. (6).

Deep in the F phase ($J \gg w_0$) all the loops are straight and winding around the system (see configuration $\mathcal{C}_F$ in Fig. 1). The relaxation time for an initial state to decay into the F ground state is bounded from below by a time of the order of the time needed by any state $|\Psi_{F,\ell \in \mathcal{C}_F}\rangle = \hat{T}_{\ell,\bar{\ell}}|\Psi_F\rangle$ to decay into the F ground state $|\Psi_F\rangle$ through spontaneous emission of phonons. The matrix element for such a quantum tunneling process is obtained from the L-th order perturbation expansion of the coupling (11), and it is therefore suppressed by an exponential factor of order $(g/U)^L$, where U is now the (large) characteristic energy scale for the three-coloring constraint and g is the typical coupling to the bath [notice that this process requires $\mathcal{O}(L)$ phonons]. Hence the relaxation time for an arbitrary initial state to decay through spontaneous emission of phonons into the F ground state is bounded from below by some positive power of $\exp(L)$.[9] The same rational applies to $\hat{H}_{RK}$.

Exponential dependence of the relaxation times on the system size is a signature of the breakdown of thermodynamic equilibration (arrested quantum dynamics). For both $\hat{H}_{RK}$ and $\hat{H}_{\mathrm{Ising}}$, it occurs in the zero temperature phase diagram of Fig. 3 as soon as the ground and first excited states belong to different topological sectors. This is a direct consequence of the fact that changing the topological sector of a given state $\otimes_{i=1}^{N}|\sigma_i^z\rangle$ requires flipping all the values of the σ_i^z (via the corresponding σ_i^x operators) along winding loops that have a length of order L. In the systems considered here, it so happens that the change in topological sector of the ground state occurs only when the system orders ferromagnetically, i.e., for sufficiently large βJ. In fact, for all $\beta J < (\beta J)_{\mathrm{cr}}$ the ground and first excited states belong to the topological sector of the AF state, i.e., the typical loops that connect the ground to the first excited states have a perimeter of order 1, and no arrested quantum dynamics is to be expected. For sufficiently large βJ the ground state belongs to the topological sector of the F state while *generic* excited states belong to different topological sectors and arrested quantum dynamics rules.

An intriguing question is what is the fate of this arrested quantum dynamics when we forbid tunneling processes between different topological sectors *before* taking the thermodynamic limit and work exclusively in the topological sector of the AF state. We believe that the mechanism for arrested quantum dynamics outlined above survives since the ground state for sufficiently large βJ should have a finite overlap with a *polycrystalline F state*, i.e., a state made of macroscopically large ferromagnetic domains in the Ising representation or one made almost exclusively of very large loops in the loop representation (see Fig. 9 of Ref. 7). Indeed, this polycrystalline F state can be obtained from a generic excited state of the AF state (characterized exclusively by small loops) only by applying σ_i^x operators along very large (though not system-spanning) loops, i.e., after the spontaneous emission of a number of phonons of order L.

Dynamical arrest is one of the characteristics of glassy systems. Classical glass formers, for example, fall out of equilibrium when the temperature is lowered and the relaxation times become of the order of the experimentally accessible time scales. In classical systems the fast decrease of the relaxational rates with decreasing temperature is associated to the increase in the times needed to surpass energy barriers by thermal activation. In quantum systems, tunneling under high (but narrow) activation barriers remains an open channel for equilibration down to zero temperature. Such quantum tunneling processes are the working principle behind the notion of *quantum annealing*,[20] which was demonstrated experimentally in the disordered Ising magnet $\mathrm{LiHo}_{0.56}\mathrm{Y}_{0.44}\mathrm{F}_4$.[21] However, quantum annealing is rendered inoperative if the tunnel barriers are *wide*, and classical thermal activation may be a more efficient thermalization process even at rather low temperatures. In this case, quantum mechanics does not prevent systems from remaining in a state of glassiness at low temperatures, very much as their classical counterparts can do in the presence of strong frustration induced by geometry or disorder.

What makes such a state of *quantum glassiness* remarkable is that it can occur in a system devoid of geometric frustration or disorder, solely as a result of strong constraints. At zero temperature, as thermal activation over energy barriers is shut down, the only mechanism for relaxation is quantum tunneling. In the quantum three-coloring model, the effective tunneling barrier widths are related to the sizes of the loops that are color-flipped. As the system tries to decay into *polycrystalline F states* with larger and larger grain sizes, tunneling of larger and larger objects is needed, and hence the relaxation rates grow exponentially with the size of the loops as long as the quantum dynamics is of a local nature. The extreme case occurs when a generic out-of-equilibrium state attempts to decay into the F state, a process that requires the exchange of the colors along loops with a perimeter of the order of the linear size of the system.

We have focused on dynamical arrest as a signature of glassy behavior. One may wonder whether a definition of a glass requires a thermodynamical transition into a glassy phase. The answer is negative, as many examples have been constructed of classical systems with trivial thermodynamics that display relaxation rates characteristic of glasses of the strong and fragile types.[22] Reference 9 provides one example of a quantum system with no thermodynamic transition but characterized by relaxation rates of a strong glass type; this system defies quantum annealing because the tunneling barriers become increasingly wide as the system effective temperature is lowered, and hence it remains in a state of quantum glassiness. The quantum three-coloring model is a second example thereof. In both cases, quantum glassiness emerges from the local nature of the Hamiltonian combined with the presence of strong constraints on the quantum dynamics.

VII. CONCLUSIONS

In this paper we have constructed a specific quantum extension $\hat{H}_{RK}$ to the three-coloring model of Baxter. Our strategy is very general as it applies to any space $\mathcal{S}$ of classical configurations $\mathcal{C}$ and to any chosen subset $\mathcal{L} \in \mathcal{S}\times\mathcal{S}$ that defines which pairs of classical configurations are related by quantum tunneling. The strategy is specific in that it demands choosing (1) a potential term $\hat{V}(\mathcal{C})$, $\forall \mathcal{C} \in \mathcal{S}$ and (2) a kinetic term $\hat{T}(\bar{\mathcal{C}},\mathcal{C})$, $\forall(\bar{\mathcal{C}},\mathcal{C}) \in \mathcal{L}$. Our choice for $\hat{H}_{RK}$ was simple in that the ground state is known for all values of two dimensionless couplings $\alpha \geqslant 0$ and $\beta J \in \mathbb{R}$. The zero-temperature phase diagram of $\hat{H}_{RK}$ as a function of $\beta J \in \mathbb{R}$ is intricate. Long-ranged ordered phases in the local Ising variables at $\beta J \ll -1$ and $\beta J \gg +1$ are separated by qualitatively different paramagnetic phases of which some are critical with respect to equal-time correlation functions. The excitation spectrum of $\hat{H}_{RK}$ depends crucially on whether $\alpha > 0$ (locality) or $\alpha = 0$ (nonlocality) and can be simulated using classical Monte Carlo methods. In the ferromagnetic phase, we have argued that the relaxation time for a generic state to decay into the ground state diverges exponentially with the system size, a trademark of quantum glassiness, when the coupling

of $\hat{H}_{RK}$ to a bath preserves the condition of locality. Thus the system prepared in a state out of equilibrium while in the ferromagnetic phase cannot decay into the exact ground state $|\Psi_{RK}\rangle$ by spontaneous emission of phonons from the bath and stalls into a mixed state however small the bath temperature is.

ACKNOWLEDGMENTS

We would like to thank C. Henley for his careful reading of this manuscript and his insightful comments. This work was supported in part by the NSF Grants DMR-0305482 and DMR-0403997 (C.C. and C.C.).

[1] D. Yoshioka, *The Quantum Hall Effect* (Springer, Berlin, 2002).
[2] X. G. Wen, *Quantum Field Theory of Many-Body Systems* (Oxford University Press, New York, 2004).
[3] S. A. Kivelson, D. S. Rokhsar, and J. P. Sethna, Phys. Rev. B **35**, 8865 (1987); D. S. Rokhsar and S. A. Kivelson, Phys. Rev. Lett. **61**, 2376 (1988); R. Moessner and S. L. Sondhi, *ibid.* **86**, 1881 (2001); C. Nayak and K. Shtengel, Phys. Rev. B **64**, 064422 (2001).
[4] R. J. Baxter, J. Math. Phys. **11**, 784 (1970).
[5] P. Di Francesco and E. Guitter, Phys. Rev. E **50**, 4418 (1994).
[6] E. N. M. Cirillo, G. Gonnella, and A. Pelizzola, Phys. Rev. E **53**, 1479 (1996).
[7] C. Castelnovo, P. Pujol, and C. Chamon, Phys. Rev. B **69**, 104529 (2004).
[8] C. L. Henley, J. Stat. Phys. **89**, 483 (1997); J. Phys.: Condens. Matter **16**, S891 (2004).
[9] C. Chamon, Phys. Rev. Lett. **94**, 040402 (2005).
[10] The three-coloring constraint on an arbitrary lattice with coordination number 3 translates to the condition that the magnetization of any closed path of the lattice is an integer multiple of 3. (Ref. 5) This is satisfied if the magnetization of any closed path of minimal length is an integer multiple of 3. When the lattice is chosen to be a planar Bravais lattice, i.e., the honeycomb lattice, the number of spins along closed paths of minimal length paths is even, namely 6, and the condition becomes that the magnetization of any elementary hexagon is 0 or ±6.
[11] N. Read, reported in Kagome workshop (Jan. 1992) (unpublished); J. Kondev and C. L. Henley, Nucl. Phys. B **464**, 540 (1996); J. Kondev, J. de Gier and B. Nienhuis, J. Phys. A **29**, 6489 (1996).
[12] E. Fradkin, D. A. Huse, R. Moessner, V. Oganesyan, and S. L. Sondhi, Phys. Rev. B **69**, 224415 (2004).
[13] Ashvin Vishwanath, L. Balents, and T. Senthil, Phys. Rev. B **69**, 224416 (2004).
[14] C. Castelnovo, C. Chamon, C. Mudry, and P. Pujol, Ann. Phys. (N.Y.) **318**, 316 (2005).
[15] E. Ardonne, P. Fendley, and E. Fradkin, Ann. Phys. (N.Y.) **310**, 493 (2004).
[16] R. Moessner, S. L. Sondhi, and P. Chandra, Phys. Rev. Lett. **84**, 4457 (2000); R. Moessner and S. L. Sondhi, Phys. Rev. B **63**, 224401 (2001).
[17] J. E. Moore and D.-H. Lee, Phys. Rev. B **69**, 104511 (2001).
[18] Xiao-Gang Wen, Phys. Rev. B **68**, 115413 (2003).
[19] A. O. Caldeira and A. J. Leggett, Ann. Phys. (N.Y.) **149**, 374 (1983).
[20] T. Kadowaki and H. Nishimori, Phys. Rev. E **58**, 5355 (1998).
[21] J. Brooke, D. Bitko, T. F. Rosenbaum, and G. Aeppli, Science **284**, 779 (1999).
[22] For a review, see F. Ritort and P. Sollich, Adv. Phys. **52**, 219 (2003).